

# Permeability of Nitric Oxide through Lipid Bilayer Membranes

WITOLD K. SUBCZYNSKI<sup>1,2</sup>, MAGDALENA LOMNICKA<sup>1</sup>, and JAMES S. HYDE<sup>2†</sup>

<sup>1</sup>Department of Biophysics, Institute of Molecular Biology, Jagiellonian University, Krakow, Poland; <sup>2</sup>Biophysics Research Institute, Medical College of Wisconsin, Milwaukee, Wisconsin, USA

Accepted by Dr. B. Kalyanaraman

(Received August 15th, 1995; in revised form, September 10th, 1995)

Profiles of the local nitric oxide ( $\bullet$ NO) diffusion-concentration product across the egg yolk phosphatidylcholine membrane in the absence and presence of 30 mol% cholesterol were obtained using line-broadening electron paramagnetic resonance (EPR) and lipid-soluble nitroxide spin labels. Membrane  $\bullet$ NO permeability coefficients were calculated from these profiles. At 20°C, values of 93 and 77 cm/s for membranes in the absence and presence of cholesterol were obtained, compared with 73 and 66 cm/s for water layers of the same thickness as the membranes. Fluid-phase membranes are not barriers to  $\bullet$ NO transport. Cholesterol significantly increases  $\bullet$ NO transport in the center of the lipid bilayer.

**Key words:** Nitric oxide, model membranes, cholesterol, membrane permeability, electron paramagnetic resonance, spin label

**Abbreviations:** EPR, electron paramagnetic resonance; EYPC, egg yolk phosphatidylcholine; 5-, 9-, 12-, and 16-SASL, 5-, 9-, 12-, and 16-doxylstearic acid spin labels; T-S, TEMPO stearate.

## INTRODUCTION

Nitric oxide ( $\bullet$ NO) serves multiple physiological functions in mammals, which have been exten-

sively investigated<sup>1–3</sup>; however, little attention has been directed to the quantitative characterization of its transport in biological systems. Information on the basic physical property of  $\bullet$ NO dealing with transport across membranes, namely the membrane permeability coefficient, is missing.<sup>4</sup>  $\bullet$ NO is one of the smallest neutral molecules and diffuses rapidly in water, nonviscous, bulk solvents and tissue.<sup>5,6</sup> It is difficult to measure the membrane permeability coefficient of  $\bullet$ NO using dynamic methods in which a fast decaying  $\bullet$ NO concentration difference across the membrane is monitored. Additional technical problems arise from the presence of a thick unmixed water layer on the surface of cells or liposomes if a fast mixing procedure is used.<sup>7</sup> To overcome these same problems in the measurement of the membrane permeability coefficient of oxygen, we developed a static method that allowed calculation of the coefficient from profiles of the oxygen diffusion-concentration product.<sup>8</sup>

<sup>†</sup>Corresponding author: James S. Hyde, Biophysics Research Institute, Medical College of Wisconsin, 8701 Watertown Plank Road, PO Box 26509, Milwaukee, WI 53266 – 0509; (414) 456 – 4000; FAX: (414) 266 – 8515; e-mail: cfelix@post.its.mcw.edu

Both  $\bullet\text{NO}$  and  $\text{O}_2$  are paramagnetic, although  $\bullet\text{NO}$  is a free radical with one unpaired electron and  $\text{O}_2$  has a triplet ground state. Both give electron paramagnetic resonance (EPR) spectra in the gaseous phase,<sup>9,10</sup> but not in solution at room temperature. Both can be observed in solution using indirect EPR methods involving nitroxide spin labels.<sup>11,12</sup> Collision of  $\bullet\text{NO}$  or  $\text{O}_2$  (unseen paramagnetic species) with nitroxide spin labels (visible EPR species) changes the EPR spectral parameters of the spin labels. This occurs because the physical interaction between these molecules involves Heisenberg spin exchange and/or dipole-dipole interaction.<sup>13</sup> This is a real physical interaction, and the method of measurement does not disturb the concentrations of colliding species. We have applied our method in the past to measure oxygen permeability across phosphatidylcholine model membranes as a function of cholesterol, carotenoid, and integral protein (bacteriorhodopsin) content as well as across the Chinese hamster ovary plasma membrane.<sup>14-17</sup>

The present report is based on the measurement of the collision rate of  $\bullet\text{NO}$  and the nitroxide fragment of the spin label. According to the Smoluchowski equation, this collision rate is proportional to the product of  $\bullet\text{NO}$  concentration and the  $\bullet\text{NO}$  diffusion coefficient in the surrounding medium. It is assumed that the diffusion coefficient of  $\bullet\text{NO}$  is much higher than that of the spin labels. The nitroxide fragment of stearic acid spin labels used by us can be placed at different depths in the membrane in the polar headgroup region as well as in the hydrocarbon region, which permits profiles of the local  $\bullet\text{NO}$  diffusion-concentration product across the lipid bilayer to be obtained. Using the procedure developed earlier for oxygen,<sup>8</sup> these profiles serve as the experimental basis for calculation of the  $\bullet\text{NO}$  membrane permeability coefficient.

Here we present results of measurements of the permeability coefficient for  $\bullet\text{NO}$  across the fluid-phase egg yolk phosphatidylcholine (EYPC) bilayer in the absence and presence of 30 mol% cholesterol. We have reached the conclusion that

the lipid bilayer portion of the biological membrane is not a barrier to  $\bullet\text{NO}$  transport. This paper complements the work of Lancaster<sup>18</sup> in which he analyzes the intra- and inter-cellular diffusion of  $\bullet\text{NO}$ .

## MATERIALS AND METHODS

### Materials

All spin labels were from Molecular Probes (Junction City, OR), EYPC from Sigma (St. Louis, MO) and cholesterol from Boehringer Mannheim. Pure argon gas was purchased from AIRCO (Murray Hill, NJ) and pure  $\bullet\text{NO}$  gas was obtained from Matheson (Joliet, IL). To ensure that all carboxyl groups of stearic acid spin labels were ionized in EYPC membranes, 0.1 M sodium borate at pH 9.5 was used as a buffer.

### Sample Preparation

The membranes used in this work were multilamellar dispersion of lipids containing 1 mol% of spin label and were prepared as described previously.<sup>8</sup> Each sample volume of 300  $\mu\text{l}$  contained  $3 \times 10^{-5}$  mol of total lipid. A special glass chamber was designed to equilibrate samples with 1 atm  $\bullet\text{NO}$  and to transfer them without contact with air and without changing the partial pressure of  $\bullet\text{NO}$  into Pasteur pipettes, which were used for EPR measurements (Figure 1). Equilibration and EPR were performed at 20°C.

### EPR Measurements

EPR spectra were obtained with a Varian E-109 X-band spectrometer. We used the linewidth of the central peak of nitroxide spin label EPR spectra, which is an NO-sensitive EPR parameter. This specific method has been applied earlier to obtain oxygen diffusion-concentration profiles across model membranes.<sup>20</sup> To obtain nitroxide line broadening due to  $\bullet\text{NO}$  collisions, two measurements are necessary: 1) The linewidth of the

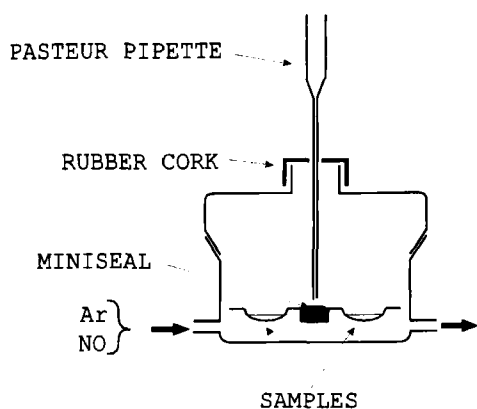


**FIGURE 1** Glass chamber designed for equilibration of samples with  $\bullet\text{NO}$ . Six samples (300  $\mu\text{l}$  each) could be equilibrated at one time. Equilibration was performed following the method of Kelm and Schrader.<sup>19</sup> The system was equilibrated for 90 min with argon, and then for 90 min with  $\bullet\text{NO}$ . This time was sufficient to fully deoxygenate samples or saturate them to equilibrium with 1 atm pressure of  $\bullet\text{NO}$ . The concentration of  $\bullet\text{NO}$  in a saturated pure water sample was 2.0 mM as verified by an ISO-NO meter from World Precision Instruments (Sarasota, FL). The end of the tube taking the gas out of the chamber was placed 10 cm under water. Pasteur pipettes could be changed without contamination of the gas inside the chamber. After insertion of a new Pasteur pipette, we allowed the gas to flow about 1 min through the pipette and then closed the end of the pipette with a rubber stopper (small septum). When the equilibration with argon or  $\bullet\text{NO}$  was completed, the bottom end of the Pasteur pipette was immersed in the sample and the top of the pipette opened. The positive pressure inside the chamber pushed the sample into the pipette, filling about 10 cm of the bottom portion. The pipette was then pushed into Miniseal wax and tightly sealed. In this way, the sample was continuously protected, not only from contact with air, but also from the changing partial pressure of  $\bullet\text{NO}$ . Only the bottom 3 cm of the sample in the Pasteur pipette was positioned in the EPR cavity and contributed to the EPR signal. The top layer ( $\sim 7$  cm) protected the "active volume" for a few hours from contact with air.

central peak of the nitroxide EPR spectrum for the sample equilibrated with argon (without  $\bullet\text{NO}$  or  $\text{O}_2$  since oxygen not only reacts with  $\bullet\text{NO}$  but also affects the EPR spectrum); and 2) the linewidth for the sample equilibrated with  $\bullet\text{NO}$ . Both are static measurements for equilibrated samples. Creation of fast decaying  $\bullet\text{NO}$  gradients is not necessary. Peak-to-peak linewidths of the central peaks were

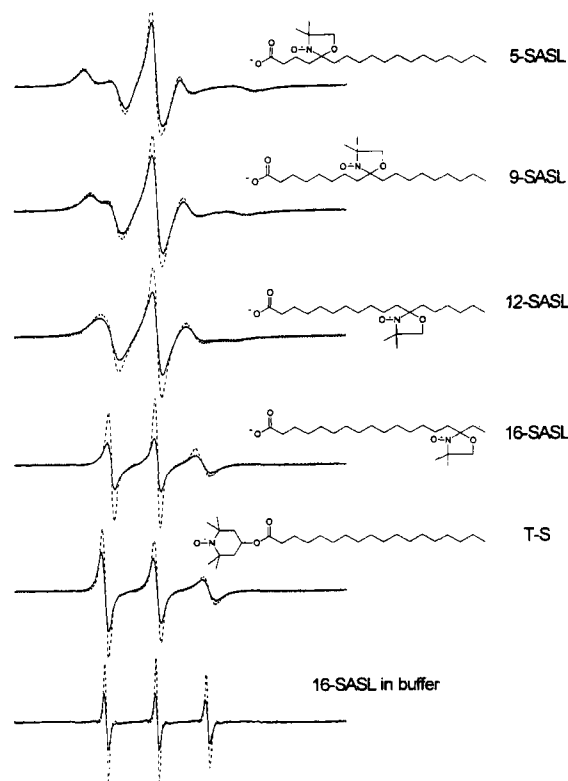


**FIGURE 2** EPR spectra from top of 5-, 9-, 12-, and 16-doxylstearic acid spin labels (5-, 9-, 12-, and 16-SASL) and TEMPO stearate (T-S) in EYPC liposome membranes and 16-SASL ( $2 \times 10^{-4}$  M) in water for sample equilibrated with argon (—) and with pure  $\bullet\text{NO}$  at 1 atm pressure (---). Chemical structures of spin labels used in this work are shown. To indicate the approximate location of the nitroxide fragment in the membrane, they are arranged according to the orientation and location in the lipid bilayer (left side, head-group region).

recorded for expanded spectra (10 G scan range) using a field modulation amplitude that was five times smaller than the linewidth.

## RESULTS AND DISCUSSION

EPR spectra for different localization of the nitroxide fragment of spin labels in the EYPC bilayer for samples equilibrated with argon and  $\bullet\text{NO}$  are shown in Figure 2. NO-induced line broadening also causes a significant decrease in the EPR signal amplitude. Figure 2 indicates that

the alkyl chain flexibility increases from the membrane surface to the membrane center.

The results of •NO-induced line broadening measured as a function of the position of the nitroxide fragment in the membrane are shown in Figure 3. These results are also expressed as the local, relative •NO diffusion-concentration product across the membrane (ratio of the local •NO diffusion-concentration product in the membrane,  $D(x)C(x)$ , to that product in water,  $D_wC_w$ ). By using the ratio, the effect of uncertainty of  $R_p$  can be reduced. Here  $p$  is the probability that an observable event is recorded when a collision takes place and  $R$  is the interaction distance. It was shown for oxygen that the product  $Rp$  is remarkably independent of solvent viscosity, temperature, and hydrophobicity.<sup>21,22</sup> For a pure lipid bilayer, the •NO diffusion-concentration product in the hydrocarbon region of the membrane is higher than in water; while in the polar headgroup region, it is about the same. Addition of cholesterol decreases the product in and near the polar headgroup region while significantly increasing it in the center of the lipid bilayer. These profiles are very similar to those obtained for oxygen in unsaturated phosphatidylcholine

membranes in the presence and absence of cholesterol.<sup>8,14</sup> Values of the •NO diffusion-concentration product in membranes equilibrated with 1 atm partial pressure of •NO at 20°C can be obtained by multiplying the ratio of  $D(x)C(x)/D_wC_w$  from Figure 3 by the product  $D_wC_w = 4.7 \times 10^{-11} \text{ mol cm}^{-1} \text{ s}^{-1}$  that was determined by classical diffusion measurement<sup>23</sup> and tables of •NO solubility in water.<sup>24</sup> Separation of  $D(x)$  and  $C(x)$  requires an independent experiment but to our knowledge, only an average •NO concentration in a pure dilauroylphosphatidylcholine bilayer can be obtained from the data presented by Singh *et al.*<sup>11</sup> The authors report only the changes in •NO concentration in the buffer after the addition of the deoxygenated suspension of dilauroylphosphatidylcholine liposomes. In the other work<sup>25</sup> the diffusion coefficient  $D = 2.7 \times 10^{-8} \text{ cm}^2 \text{ s}^{-1}$  of •NO in the fluid-phase dimyristoylphosphatidylcholine bilayer is reported (an unrealistically low value) based on phosphorescence quenching measurements and the assumption that •NO solubility in the lipid bilayer is the same as in hydrocarbon solvents.

The rate of all chemical reactions involving •NO depends on the collision frequency of •NO with attacked molecules and, thus, on the local •NO diffusion-concentration product. It can be inferred that chemical reactions of •NO with oxygen or lipid peroxy radicals will proceed more readily in the membrane center than in the membrane regions close to its surface. However, in membranes, •NO is protected against reactions with water-soluble compounds, which significantly limit its diffusion.<sup>26</sup> Membranes could be considered as short-time storage environments for •NO within the cell that supplement the long time NO-buffering provided by plasma S-nitrosothiols.<sup>27,28</sup> Furthermore, according to the hypothesis of Skulachev,<sup>29</sup> the extended membranous system may provide routes for intracellular •NO transport. •NO transport across the polar cytosol seems likely to be less effective.

Based on the profiles presented in Figure 3, the membrane permeability coefficients for •NO,  $P_M$ ,

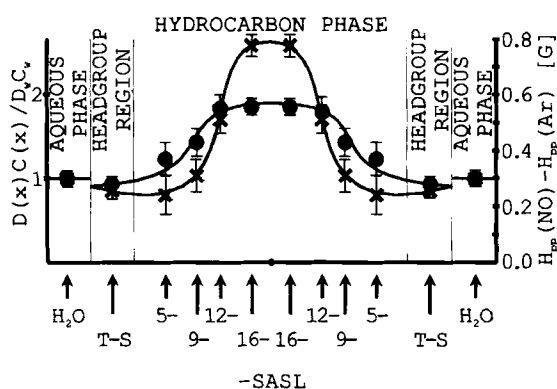


FIGURE 3 Profiles of the relative •NO diffusion-concentration product (or •NO induced EPR line broadening) across EYPC bilayer in the absence (—●—) and presence (---X---) of 30 mol% cholesterol at 20°C. The approximate locations of nitroxide fragments of spin labels are indicated by arrows. Data for aqueous phase (indicated by ↑H<sub>2</sub>O) were obtained with 16-SASL, which at pH 9.5 is fairly soluble in water. Data points represented mean ± S.D. (n = 4).

TABLE 1 •NO and O<sub>2</sub> permeability coefficients for EYPC-cholesterol membranes at 20°C.

Solute	Cholesterol mol fraction (%)	$D_W^a$ (10 <sup>-5</sup> cm <sup>2</sup> /s)	$P_W^b$ (cm/s)	$P_M/P_W^c$ from line- broadening EPR	$P_M^d$ (cm/s)
•NO	0.0	2.35	73.0	1.28	93.0
•NO	30.0	2.35	66.0	1.17	77.0
O <sub>2</sub>	0.0	2.00	62.0	1.08	67.0
O <sub>2</sub>	27.5	2.00	56.0	0.85	48.0

<sup>a</sup>The bulk diffusion coefficient,  $D_W$ , of •NO and O<sub>2</sub> in water. Data obtained from<sup>23</sup> for •NO and from<sup>30</sup> for oxygen.

<sup>b</sup>•NO and O<sub>2</sub> permeability coefficients,  $P_W$ , in a water layer of the same thickness as the membrane calculated from  $D_W$  and membrane thickness,  $\delta_M$ , according to Eq.:  $P_W = D_W/\delta_M$ .

<sup>c</sup>The ratio was determined from  $P_M$  and  $P_W$ , both of which were determined in the EPR line-broadening experiment.

<sup>d</sup> $P_M$  was determined by multiplying  $P_W$  determined from the bulk-diffusion coefficient and the  $P_M/P_W$  ratio determined by the present spin-label method. In this way, methodological uncertainty is reduced.

Membrane thicknesses,  $\delta_M$ , were obtained as described previously<sup>8,14</sup> and were for pure EYPC 32.1 Å and for EYPC 30 mol% cholesterol 35.8 Å. It was assumed that the location of the alkyl chain carbon atoms in the membrane changes linearly with the position on the alkyl chain (the maximum error is about  $\pm 1.5$  Å<sup>31</sup> and that the nitroxide fragment of SASL is located at the mean depth of the 1- and 2-chain of EYPC.

were calculated using the procedure described earlier (Table 1).<sup>8,14,15,17</sup> It was assumed that •NO diffusion within the lipid bilayer is isotropic. It has been previously shown that oxygen diffusion (which should resemble •NO diffusion very well) is almost isotropic in the fluid-phase of non-cholesterol-containing membranes.<sup>32</sup> Diffusion of oxygen below the pretransition temperature was found to be more rapid in the transverse than in the lateral direction. For comparison, values of the oxygen permeability coefficients from Ref. 14 have been included in Table 1. At 20°C, pure unsaturated phosphatidylcholine membrane, which at this temperature is in the fluid phase, is not a barrier to •NO permeation. Addition of cholesterol (30 mol%) to the phospholipid bilayer decreases the permeability coefficient. However, effects of cholesterol on the •NO diffusion-concentration product in the membrane center and close to the membrane surface tend to cancel, resulting in only a moderate net effect of cholesterol on the permeability coefficient. At physiological temperatures, the ratio of  $P_M/P_W$  should increase.  $P_W$  (the •NO permeability coefficient in a water layer of the same thickness as the membrane) does not change significantly with temperature because the temperature dependencies of

•NO diffusion and concentration are opposite.<sup>23,24</sup>

$P_M$ , however, should significantly increase because increase of temperature not only increases the diffusion of •NO, but also the partition coefficient of •NO between hydrocarbons and water.<sup>33</sup>

The membrane is a permeability barrier to •NO if  $P_M/P_W < 1$ , but not if  $P_M/P_W > 1$ . Our data indicate that EYPC bilayer without and with cholesterol is not a barrier to •NO permeation. Because EYPC is a natural phospholipid containing alkyl chains of different length and degree of unsaturation, and because cholesterol is a common component of mammalian cell membranes, we think that we can extend our conclusion to the lipid portion of biological membranes of mammalian organisms.

Apparently, no measurements of the •NO membrane permeability coefficient have been made previously. Several data do exist based on the assumption that •NO partitioning into the lipid bilayer is constant across the entire membrane thickness and is the same as •NO partitioning into octanol or hexadecane.<sup>5,34</sup> It is customary to assume that partition coefficients of small nonelectrolytes between organic solvents and water are similar to those for lipid bilayers. Direct



support for this assumption, however, is lacking. Moreover, a number of studies based on radioactive isotope labeling or molecular probe measurement report that the average partitioning of noble gases, carbon dioxide or oxygen in anisotropic organized media such as lipid bilayers is much lower than in isotropic media such as hexane, octanol, or olive oil.<sup>35-39</sup>

Additionally, it is not possible to evaluate the membrane permeability coefficient of •NO from a single (average) value of the •NO diffusion coefficient and a single (average) value of the •NO concentration (or partition coefficient). This conclusion follows from the theory of Diamond and Katz for permeation of nonelectrolytes across the membrane<sup>40</sup> and from the profiles of the diffusion-concentration product across the membrane obtained by us for •NO in the present work and earlier for oxygen.<sup>8,14,20</sup> Both change significantly from the membrane surface to the membrane center. The integration of  $(C(x)D(x))^{-1}$ , which is a measure of resistance to •NO permeation, over the entire thickness of the lipid bilayer is necessary.<sup>8,14,15,17</sup>

Our approach yields answers to two fundamental questions about •NO permeation through lipid bilayers. 1) Can a membrane be a permeability barrier for •NO, and 2) if so, what is the location of the major permeability resistance? Classical methods give the permeability coefficient as an average property of the membrane without distinguishing regions of high or low solute transport. A small permeability resistance to •NO is induced by cholesterol in and near the polar headgroups, but resistance decreases in the membrane center. Oxygen permeability across the EYPC bilayer is affected more strongly by cholesterol because it significantly decreases the oxygen diffusion-concentration product in and near the polar headgroup region. Cholesterol significantly increases the polarity of this region to the depth of 7–9 carbons in alkyl chains.<sup>41</sup> This affects the solubility of oxygen more strongly than that of •NO, because •NO is more polar. The dipole moment of •NO is 0.159 D; for oxygen, it

is zero.<sup>24</sup> This property gives a slightly higher solubility to •NO in polar solvents and, as measured by us, a slightly higher diffusion-concentration product. In hydrophobic solvents, such as octanol or paraffin oil, the diffusion-concentration product of O<sub>2</sub> is higher than for •NO (for the same partial pressure of both gases). Our data confirm the statement that •NO and O<sub>2</sub> resemble each other in transport properties.

Previously,<sup>17</sup> we showed that the equation  $P_M = cK^s$ , where  $P_M$  is the EYPC membrane permeability of a nonelectrolyte and  $K$  is the partition coefficient into hexane, is valid for nonelectrolyte solutes of mol wt < 50 using  $c = 26$  cm/s,  $s = 0.95$ . •NO data satisfy this equation using values of  $P_M$  reported here and values of  $K$  from tables of •NO solubility in hydrocarbons.<sup>33</sup>

Two molecular probe techniques have been introduced to measure the frequency of collision between the probe and •NO; phosphorescence quenching<sup>25,42</sup> and EPR spin-label line broadening.<sup>11</sup> Both were applied to study •NO transport in synthetic phospholipid bilayers. During the past 15 years, we have developed and applied spin-label oximetry.<sup>12</sup> We believe that spin-label NO-metry will provide an understanding of •NO transport in complex biological systems analogous to spin-label oximetry.

### Acknowledgements

This work was supported in part by grants GM22923 and RR01008 from the US National Institutes of Health. Partial support from Jagiellonian University is appreciated.

### References

1. S. Moncada, R.M.J. Palmer and E.A. Higgs (1991) Nitric oxide: physiology, pathophysiology, and pharmacology. *Pharmacological Review*, **43**, 109–142.
2. C. Nathan (1992) Nitric oxide as a secretory product of mammalian cells. *FASEB Journal*, **43**, 3051–3064.
3. P.L. Feldman, O.W. Griffith and D.J. Stuehr (1993) The surprising life of nitric oxide. *Chemical and Engineering News*, December 20, pp. 26–38.
4. J.S. Stamler, D.J. Singel and J. Loscalzo (1992) Biochemistry of nitric oxide and its redox-activated forms. *Science*, **258**, 1898–1902.
5. T. Malinski, Z. Taha and S. Grunfeld (1993) Diffusion of nitric oxide in the aorta wall. *Biochemical and Biophysical Research Communications*, **193**, 1076–1082.

6. A. Meulemans (1994) Diffusion coefficients and half-lives of nitric oxide and N-nitroso-L-arginine in rat cortex. *Neuroscience Letters*, **171**, 89–93.
7. V.H. Huxley and M.J. Kutchai (1983) Effects of diffusion boundary layers on the initial uptake of oxygen by red blood cells: theory vs experiments. *Microvascular Research*, **26**, 89–107.
8. W.K. Subczynski, J.S. Hyde and A. Kusumi (1989) Oxygen permeability of phosphatidylcholine-cholesterol membranes. *Proceedings of the National Academy of Sciences, USA*, **86**, 4474–4478.
9. A. Carrington, D.H. Levy, T.A. Miller and J.S. Hyde (1967) Double quantum transitions in gas-phase electron resonance. *Journal of Chemical Physics*, **47**, 4859–4860.
10. R. Beringer and J.G. Castle, Jr. (1951) Microwave magnetic resonance spectrum of oxygen. *Physical Review*, **81**, 82–88.
11. R.J. Singh, N. Hogg, H.S. Mchaourab and B. Kalyanaram (1994) Physical and chemical interactions between nitric oxide and nitroxides. *Biochimica et Biophysica Acta*, **1201**, 437–441.
12. J.S. Hyde and W.K. Subczynski (1989) Spin-label oximetry. In: *Biological Magnetic Resonance. Spin Labeling: Theory and Applications*, Vol. 8 (Eds., L.J. Berliner and J. Reuben) Plenum, New York, pp. 399–425.
13. Y.N. Molin, K.M. Salkhov and K.I. Zamaraev (1980) *Spin Exchange*. Springer, New York.
14. W.K. Subczynski, J.S. Hyde and A. Kusumi (1991) Effect of alkyl chain unsaturation and cholesterol intercalation on oxygen transport in membranes: a pulse ESR spin labeling study. *Biochemistry*, **30**, 8578–8590.
15. W.K. Subczynski and E. Markowska (1992) Effect of carotenoids on oxygen transport within and across model membranes. *Current Topics in Biophysics*, **16**, 62–68.
16. I. Ashikawa, J.-J. Yin, W.K. Subczynski, T. Kouyama, J.S. Hyde and A. Kusumi (1994) Molecular organization and dynamics in bacteriorhodopsin-rich reconstituted membranes: discrimination of lipid environment by the oxygen transport parameter using a pulse ESR spin-labeling technique. *Biochemistry*, **33**, 4947–4952.
17. W.K. Subczynski, L.E. Hopwood and J.S. Hyde (1992) Is the cell plasma membrane a barrier to oxygen transport? *Journal of General Physiology*, **100**, 68–87.
18. J.R. Lancaster, Jr. (1994) Simulation of the diffusion and reaction of endogenously produced nitric oxide. *Proceedings of the National Academy of Sciences, USA*, **91**, 8137–8141.
19. M. Kelm and J. Schrader (1990) Control of coronary vascular tone by nitric oxide. *Circulation Research*, **66**, 1561–1575.
20. D.A. Windrem and W.Z. Plachy (1980) The diffusion-solubility of oxygen in lipid bilayers. *Biochimica et Biophysica Acta*, **600**, 655–665.
21. J.S. Hyde and W.K. Subczynski (1984) Simulation of ESR spectra of the oxygen-sensitive spin-label probe CTPO. *Journal of Magnetic Resonance*, **56**, 125–130.
22. W.K. Subczynski and J.S. Hyde (1984) Diffusion of oxygen in water and hydrocarbons using an electron spin resonance spin-label technique. *Biophysical Journal*, **45**, 743–748.
23. D. R. Lide, ed. (1990–1991) *Handbook of Chemistry and Physics*, 71st ed. CRC Press, Boca Raton, p. 6–151.
24. D.R. Lide, ed. (1992–1993) *Handbook of Chemistry and Physics*, 73rd ed. CRC Press, Boca Raton, pp. 6–4, 9–55.
25. J.M. Vanderkooi, W.W. Wright and M. Erecinska (1994) Nitric oxide diffusion coefficients in solutions, proteins, and membranes determined by phosphorescence. *Biochimica et Biophysica Acta*, **1207**, 249–254.
26. V.G. Kharitonov, A.R. Sundquist and V.S. Sharma (1994) Kinetics of nitric oxide autooxidation in aqueous solution. *Journal of Biological Chemistry*, **269**, 5881–5883.
27. K. Aisaka, S.S. Gross, O.W. Griffith and R. Levi (1989) L-arginine availability determines the duration of acetylcholine-induced systemic vasodilation *in vivo*. *Biochemical and Biophysical Research Communications*, **163**, 710–717.
28. J.S. Stamler, O. Jaraki, J.A. Osborne, D.I. Simons, J. Vita, D. Singel, C.R. Valeri and J. Localzo (1992) Nitric oxide circulates in mammalian plasma primarily as an S-nitroso adduct of serum albumin. *Proceedings of the National Academy of Sciences, USA*, **89**, 7674–7677.
29. V.P. Skulachev (1990) Power transmission along biological membranes. *Journal of Membrane Biology*, **114**, 97–112.
30. C.E. St.-Denis and C.J.D. Fell (1971) Diffusivity of oxygen in water. *Canadian Journal of Chemical Engineering*, **49**, 885.
31. G. Zaccai, G. Buldt, A. Seelig and J. Seelig (1979) Neutron diffraction studies on phosphatidylcholine model membranes: chain conformation and segmental disorder. *Journal of Molecular Biology*, **134**, 693–706.
32. A. Kusumi, W.K. Subczynski and J.S. Hyde (1982) Oxygen transport parameter in membranes as deduced by saturation recovery measurements of spin-lattice relaxation times of spin labels. *Proceedings of the National Academy of Sciences, USA*, **79**, 1854–1858.
33. W.F. Linke (1965) *Solubilities, Inorganic and Metal-Organic Compounds*, Vol. 2 4th ed. American Chemical Society, Washington, DC, p. 792.
34. J. Goretzki and T.C. Hollocher (1988) Trapping of nitric oxide produced during denitrication by extracellular hemoglobin. *Journal of Biological Chemistry*, **263**, 2316–2323.
35. G.G. Power and H. Stegall (1970) Solubility of gases in human red blood cell ghosts. *Journal of Applied Physiology*, **29**, 145–149.
36. Y. Katz and S.A. Simon (1977) Physical parameters of the anesthetic site. *Biochimica et Biophysica Acta*, **471**, 1–15.
37. S.A. Simon and J. Gutknecht (1980) Solubility of carbon dioxide in lipid bilayer membranes and organic solvents. *Biochimica et Biophysica Acta*, **596**, 352–358.
38. W.K. Subczynski and J.S. Hyde (1983) Concentration of oxygen in lipid bilayers using a spin-label method. *Biophysical Journal*, **41**, 283–286.
39. E.S. Smotkin, F.T. Moy and W.K. Plachy (1991) Dioxygen solubility in aqueous phosphatidylcholine dispersion. *Biochimica et Biophysica Acta*, **1061**, 33–38.
40. J.M. Diamond and Y. Katz (1974) Interpretation of non-electrolyte partition coefficients between dimyristoyl lecithin and water. *Journal of Membrane Biology*, **17**, 121–154.
41. W.K. Subczynski, A. Wisniewska, J.-J. Yin, J.S. Hyde and A. Kusumi (1994) Hydrophobic barriers of lipid bilayer membranes formed by reduction of water penetration by alkyl chain unsaturation and cholesterol. *Biochemistry*, **33**, 7670–7681.
42. G.B. Stambini (1987) Quenching of alkaline phosphatase phosphorescence by O<sub>2</sub> and NO. Evidence for inflexible regions of protein structure. *Biophysics Journal*, **52**, 23–28.